ITALIAN PHYSICAL SOCIETY

PROCEEDINGS

OF THE

INTERNATIONAL SCHOOL OF PHYSICS

«ENRICO FERMI»

COURSE CXVII

edited by A. STELLA

Director of the Course

and by

L. MIGLIO

Scientific Secretary

VARENNA ON LAKE COMO

VILLA MONASTERO

25 June - 5 July 1991

Semiconductor Superlattices and Interfaces

1993

NORTH-HOLLAND

AMSTERDAM - OXFORD - NEW YORK - TOKYO

Thermal and Thermo-Electric Transport Properties of Quantum Point Contacts.

L. W. MOLENKAMP, H. VAN HOUTEN and C. W. J. BEENAKKER

Philips Research Laboratories - 5600 JA Eindhoven, The Netherlands

C. T. FOXON (*)

Philips Research Laboratories - Redhill, Surrey RH1 5HA, United Kingdom

1. – Introduction.

A quantum point contact (QPC) is a short constriction of variable width, comparable to the Fermi wavelength, usually defined using a split-gate technique in a high-mobility two-dimensional electron gas (2DEG). QPC's are best known for their quantized conductance at integer multiples of $2e^2/h$ [1-3]. In addition, they have proven to be versatile probes for the study of electrical conduction in the ballistic and quantum Hall effect regime [3]. Recently, we have used QPC's in studies of thermal conduction and of thermo-electric cross-phenomena. Our results are reviewed in this lecture.

Electrical conduction in linear response can be understood using the Landauer-Büttiker formalism [4, 5], which relates the conduction to transmission probabilities. This scattering formalism has been generalized to thermal and thermo-electric transport properties by SIVAN and IMRY [6] and by BUTCHER [7]. STREDA [8] has considered specifically the problem of the thermopower of a QPC. He found that the thermopower vanishes whenever the conductance of the point contact is quantized, and that it exhibits peaks between plateaux of quantized conductance. Within this theoretical framework one can show that the thermal conductance κ and the Peltier coefficient Π should exhibit quantum size effects similar to those in the conductance G and the thermopower S, respectively. We review the theory in sect. 2.

(*) Present address: Department of Physics, University of Nottingham, Nottingham NG7 2RD, U.K.

An experimental difficulty in the investigation of thermal and thermo-electric properties in the ballistic transport regime is that appreciable temperature differences have to be created on a length scale of the mean free path, which is a few μm. A current heating technique [9] has enabled us to realize temperature differences on such short length scales. Our work on the quantum oscillations in the thermopower [10, 11] is reviewed in subsect. 3·1. Because of the sizable thermopower, a QPC can be used as a miniature thermometer, to probe the local temperature of the electron gas. We have exploited this in a series of novel devices containing multiple QPC's, with which we demonstrate quantum steps in the thermal conductance as well as quantum oscillations in the Peltier coefficient of a QPC. The results of these experiments are presented in subsect. 3·2 and 3·3. Concluding remarks are given in sect. 4. The text of this lecture is based on ref. [12], updated to include improved experimental results on the Peltier coefficient.

2. – Theoretical background.

2·1. *Scattering formalism for thermo-electricity.* – We consider the electrical current I and heat current Q between two reservoirs at electrochemical potentials E_F and $E_F + \Delta\mu$ and temperatures T and $T + \Delta T$. For small differences $\Delta\mu$ and ΔT the currents I and Q satisfy the linear matrix equations [13]

$$\begin{pmatrix} I \\ Q \end{pmatrix} = \begin{pmatrix} G & L \\ M & K \end{pmatrix} \begin{pmatrix} \Delta\mu/e \\ \Delta T \end{pmatrix}. \tag{1}$$

The thermo-electric coefficients L and M are related by an Onsager relation, which in the absence of a magnetic field is

$$M = -LT. \tag{2}$$

Equation (1) is often rearranged with the current I rather than the electrochemical potential difference $\Delta\mu$ on the right-hand side [13]:

$$\begin{pmatrix} \Delta\mu/e \\ Q \end{pmatrix} = \begin{pmatrix} R & S \\ \Pi & -\kappa \end{pmatrix} \begin{pmatrix} I \\ \Delta T \end{pmatrix}. \tag{3}$$

The resistance $R = 1/G$ is the reciprocal of the conductance G. The thermopower S is defined as

$$S \equiv \left(\frac{\Delta\mu/e}{\Delta T} \right)_{I=0} = -L/G. \tag{4}$$

The Peltier coefficient Π, defined as

$$\Pi \equiv \left(\frac{Q}{I} \right)_{\Delta T=0} = M/G = ST, \tag{5}$$

is proportional to the thermopower in view of the Onsager relation (2). Finally, the thermal conductance κ is defined as

$$\kappa \equiv -\left(\frac{Q}{\Delta T}\right)_{I=0} = -K\left(1 + \frac{S^2 GT}{K}\right). \tag{6}$$

The term between brackets in eq. (6) is usually close to unity.

The thermal and thermo-electric coefficients were related to the transmission probabilities for a multi-terminal geometry in ref. [6] and [7]. Here we will only use the two-terminal expressions, for which the derivation is outlined in the appendix. We find the following expressions:

$$G = -\frac{2e^2}{h}\int_0^\infty \mathrm{d}E\,\frac{\partial f}{\partial E}\,t(E), \tag{7}$$

$$L = -\frac{2e^2}{h}\,\frac{k_B}{e}\int_0^\infty \mathrm{d}E\,\frac{\partial f}{\partial E}\,t(E)\,\frac{E - E_F}{k_B T}, \tag{8}$$

$$\frac{K}{T} = \frac{2e^2}{h}\left(\frac{k_B}{e}\right)^2 \int_0^\infty \mathrm{d}E\,\frac{\partial f}{\partial E}\,t(E)\left(\frac{E - E_F}{k_B T}\right)^2. \tag{9}$$

These integrals are convolutions of the total transmission probability $t(E)$ at energy E through a kernel of the form $\varepsilon^m \mathrm{d}f/\mathrm{d}\varepsilon$, $m = 0, 1, 2$, with $\varepsilon \equiv (E - E_F)/k_B T$, and f the Fermi function

$$f(\varepsilon) = (\exp[\varepsilon] + 1)^{-1}. \tag{10}$$

Plots of these kernels are given in fig. 1.

The conductance and thermal conductance are approximately proportional to $t(E_F)$, while the thermo-electric cross-coefficients are approximately proportional to the derivative $\mathrm{d}t(E)/\mathrm{d}E$ at $E = E_F$. This follows from a Sommerfeld expansion of the integrals (7)-(9), valid for a smooth function $t(E)$ to lowest order in $k_B T/E_F$ [7]:

$$G \approx \frac{2e^2}{h}\,t(E_F), \tag{11}$$

$$L \approx \frac{2e^2}{h}\,L_0 eT\left(\frac{\mathrm{d}t(E)}{\mathrm{d}E}\right)_{E=E_F}, \tag{12}$$

$$K \approx -\frac{2e^2}{h}\,L_0 T t(E_F). \tag{13}$$

Here $L_0 \equiv k_B^2 \pi^2/3e^2$ is the Lorentz number. In this approximation $K = -L_0 TG$,

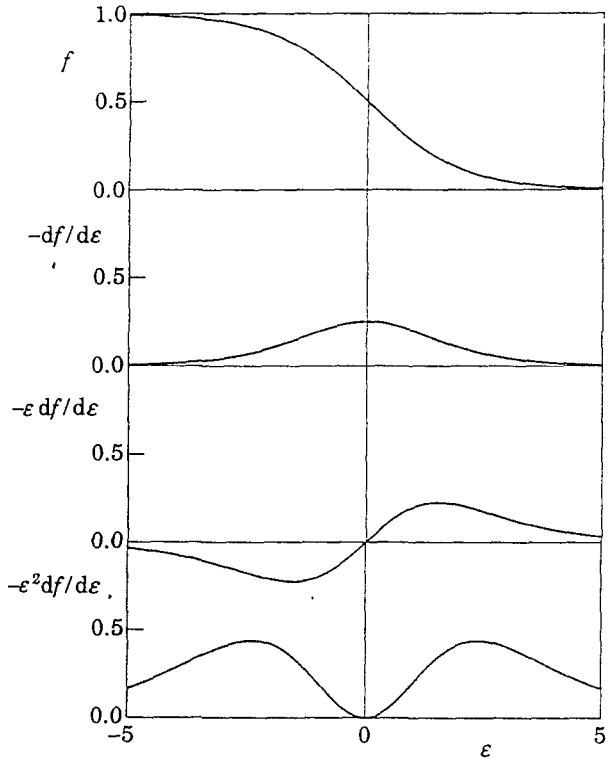

Fig. 1. – From top to bottom: Fermi-Dirac distribution function f, and $\varepsilon^m \mathrm{d}f/\mathrm{d}\varepsilon$, for $m = 0$, 1, 2, as a function of $\varepsilon \equiv (E - E_F)/k_B T$. These functions appear in the expressions (7)-(9) for the transport coefficients.

so that for $S^2 \ll L_0$ one finds from (6) the Wiedemann-Franz relation

$$\kappa \approx L_0 TG . \tag{14}$$

As discussed below, the thermal and thermo-electric coefficients of a QPC may exhibit significant deviations from eqs. (12)-(14). The inadequacy of the Sommerfeld expansion is a consequence of the strong energy dependence of $t(E)$ near E_F. In addition, $S^2 \ll L_0$ does not hold for a QPC close to pinch-off.

2·2. *Quantum point contact as ideal electron waveguide.* – In this subsection we calculate the thermal and thermo-electric properties of a QPC by modelling it as an ideal electron waveguide, which is coupled reflectionless to the reservoirs at entrance and exit. In this model the transmission probability has a step-function energy dependence

$$t(E) = \sum_{n=1}^{\infty} \theta(E - E_n) . \tag{15}$$

The steps in $t(E)$ occur at the threshold energies E_n of the one-dimensional subbands or modes in the waveguide. The energy integrals in eqs. (7) and (8) for the conductance and the thermopower can be evaluated analytically. By substitution of eq. (15) into eq. (7), one finds for the conductance

$$G = \frac{2e^2}{h} \sum_{n=1}^{\infty} f(\varepsilon_n), \tag{16}$$

with $\varepsilon_n \equiv (E_n - E_F)/k_B T$. This reduces to $G = (2e^2/h)N$ at low temperatures (N is the number of occupied subbands at energy E_F). Similarly, using the identity

$$\int_0^{\infty} f \mathrm{d}E = k_B T \ln(1 + \exp[E_F/k_B T]), \tag{17}$$

we find

$$L = \frac{2e^2}{h} \frac{k_B}{e} \sum_{n=1}^{\infty} [\ln(1 + \exp[-\varepsilon_n]) + \varepsilon_n (1 + \exp[\varepsilon_n])^{-1}]. \tag{18}$$

The thermopower $S = -L/G$ and the Peltier coefficient $\Pi = TS = -TL/G$ follow immediately from eqs. (16) and (18). At low temperatures the thermopower vanishes, unless the Fermi energy is within $k_B T$ from a subband bottom. In the limit $T = 0$ one finds from eqs. (16) and (18) that the maxima are given by

$$S = -\frac{k_B}{e} \frac{\ln 2}{N - 1/2}, \qquad \text{if } E_F = E_N, \quad N \geq 2. \tag{19}$$

(Note that at $E_F = E_N$ one also has $G = (2e^2/h)(N - 1/2)$.) Equation (19) was first obtained by STREDA [8]. For this ideal waveguide model the width of the peaks in the thermopower as a function of E_F is of order $k_B T$, as long as $\Delta T \ll T$.

Plots of the transport coefficients as a function of Fermi energy, calculated from eqs. (7)-(9) and (15), are given in fig. 2 for $T = 1$ K. The values for E_n are those for a parabolic lateral confinement potential $V(y) = V_0 + (1/2)m\omega_y^2 y^2$, with $\hbar\omega_y = 2.0$ meV. We draw the following conclusions from these calculations. 1) The temperature T affects primarily the width of the steps in G and of the peaks in S, leaving the value of G on the plateaux, and the height of the peaks in S essentially unaffected. 2) The thermal conductance κ (divided by $L_0 T$) exhibits secondary plateaux near the steps in G, in violation of the Wiedemann-Franz law. At 4 K the secondary plateaux in κ are even more pronounced than those which line up with the plateaux in the conductance. These secondary plateaux are due to the bimodal shape of the kernel $\varepsilon^2 \mathrm{d}f/\mathrm{d}\varepsilon$ (see fig. 1). 3) The difference between κ and K (cf. eq. (6)) is usually negligible, except in the vicinity of the first step in G.

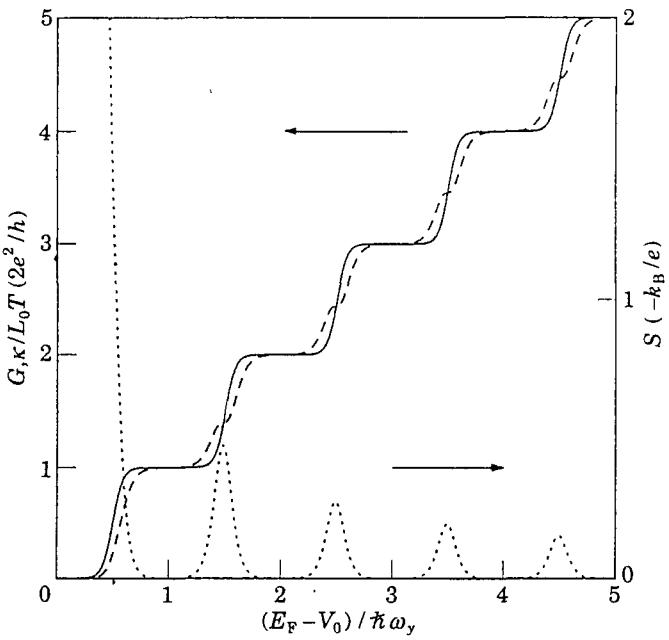

Fig. 2. – Calculated conductance G (full curve), thermal conductance κ/L_0T (dashed curve) and thermopower S (dotted curve) for a QPC with step function $t(E)$ as a function of Fermi energy at 1 K. The Peltier coefficient $\Pi = TS$ differs only by a constant factor from S. A parabolic confinement was assumed in the QPC, with subband splitting $\hbar\omega_y = 2\,\text{meV}$.

3. – Experiments.

3·1. *Thermopower.* – We have previously reported [10, 11] the observation of quantum oscillations in the thermopower of a QPC using a current heating technique. We review the main results here. The experimental arrangement is shown schematically in fig. 3*a*). By means of negatively biased split gates, a channel is defined in the 2DEG in a GaAs-AlGaAs heterostructure. A quantum point contact is incorporated in each channel boundary. The point contacts 1 and 5 face each other, so that the transverse voltage $V_1 - V_5$ (measured using Ohmic contacts attached to the 2DEG regions behind the point contacts) does not contain a contribution from the voltage drop along the channel.

On passing a current I through the channel, the average kinetic energy of the electrons increases, because of the dissipated power (equal to $(I/W_{ch})^2\,\varrho$ per unit area, for a channel of width W_{ch} and resistivity ϱ). We have experimental evidence that the net drift velocity in the channel between the QPC's is not essential for the transverse voltage [10]. We, therefore, ignore this drift velocity and model the distribution function in the channel by a heated Fermi function at

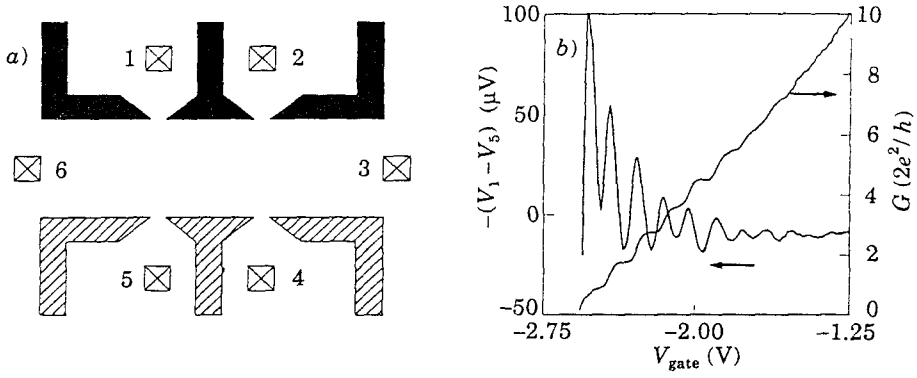

Fig. 3. – *a*) Layout of the device used to demonstrate quantum oscillations in the thermopower of a QPC by means of a current heating technique. The channel has a width of 4 μm, and the two opposite quantum point contacts at its boundaries are adjusted differently. *b*) Measured conductance and transverse voltage $-(V_1 - V_5)$ as a function of the gate voltage defining point contact 1 (black gates), at a lattice temperature of 1.65 K and a current of 5 μA. The gates defining point contact 2 (dashed) were kept at – 2.0 V.

temperature $T + \Delta T$. This temperature difference ΔT gives rise to a thermovoltage

$$V_1 - V_5 = (S_1 - S_5)\,\Delta T. \tag{20}$$

As dictated by the symmetry of the channel (see fig. 3*a*)), this transverse voltage vanishes unless the point contacts have unequal thermopowers $S_1 \neq S_5$.

A typical experimental result [10] is shown in fig. 3*b*). In the experiments, the gate voltage on the black-painted gates in fig. 3*a*) (which define point contact 1) is varied, while the voltage on the hatched gates (defining point contact 5) is kept constant. In this way, any change in the transverse voltage $V_1 - V_5$ is due to variations in S_1. (S_5 is not negligible in this experiment, which is why the trace for $-(V_1 - V_5)$ drops below zero in fig. 3*b*).) Also shown is the conductance G of point contact 1, obtained from a separate measurement. We observe strong oscillations in $V_1 - V_5$. The peaks occur at gate voltages where G changes stepwise because of a change in the number of occupied 1D subbands in point contact 1. These are the quantum oscillations of the thermopower predicted by STREDA [8].

A detailed comparison of the oscillations in fig. 3*b*) with the ideal electron waveguide model (extended to the regime of finite thermovoltages and temperature differences) has been presented elsewhere [10]. The decrease in amplitude of consecutive peaks is in agreement with eq. (19). The largest peak near $G = 1.5(2e^2/h)$ has a measured amplitude of about 75 μV. The theoretical result eq. (19) predicts $S \approx -40\,\mu V/K$ for this peak, which indicates that the temperature of the electron gas in the channel is $\Delta T \approx 2$ K above the lattice temperature $T = 1.65$ K.

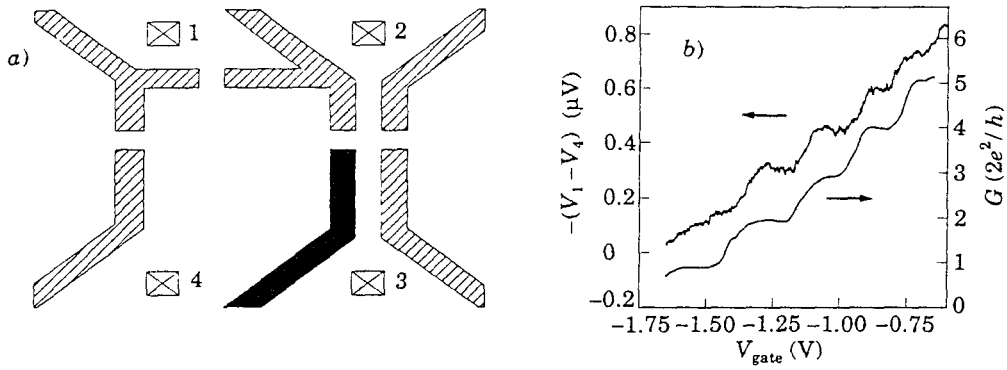

Fig. 4. – *a*) Layout of the device used to demonstrate quantum steps in the thermal conductance of a QPC, using another point contact as a miniature thermometer. The main channel is 0.5 μm wide. *b*) Measured conductance and r.m.s. value of the second-harmonic component of the voltage $-(V_1 - V_4)$ as a function of the gate voltage defining the point contact in the main channel boundary (black gate), at a lattice temperature of 1.4 K and an alternating current of r.m.s. amplitude 0.6 μA. The gates defining the other point contact (dashed) were kept at − 1.4 V, so that its conductance was $G = 1.5(2e^2/h)$.

We relate the increase in electron temperature to the current in the channel by the heat balance equation

$$c_v \Delta T = (I/W_{ch})^2 \rho \tau_\varepsilon \,, \tag{21}$$

with $c_v = (\pi^2/3)(k_B T/E_F) n_s k_B$ the heat capacity per unit area, n_s the electron sheet density, and τ_ε an energy relaxation time associated with energy transfer from the electron gas to the lattice. The symmetry of the geometry implies that $V_1 - V_5$ should be even in the current, and eq. (21) implies more specifically that the thermovoltage difference $V_1 - V_5 \propto \Delta T$ should be proportional to I^2—at least for small current densities. This agrees with our experiments [10, 11] (not shown). Equation (21) allows us to determine the relaxation time τ_ε from the value $\Delta T \sim 2$ K deduced from our experiment. Under the experimental conditions of fig. 3*b*) we have $T = 1.65$ K, $I = 5\,\mu$A, $W_{ch} = 4\,\mu$m, $\rho = 20\,\Omega$. We thus find $\tau_\varepsilon \sim 10^{-10}$ s, which is not an unreasonable value for the 2DEG in GaAs-AlGaAs heterostructures at helium temperatures [14].

3·2. *Thermal conductance.* – The sizable thermopower of a QPC (up to − 40 μV/K) suggests its possible use as a miniature thermometer, suitable for local measurements of the electron gas temperature. We have used this idea to measure with one QPC the quantum steps in the thermal conductance of another QPC.

The geometry of the device is shown schematically in fig. 4*a*). The main channel has a boundary containing a QPC. Using current heating, the electron gas temperature in the channel is increased by ΔT, giving rise to a heat flow Q

through the point contact. This causes a much smaller temperature rise δT of the 2DEG region behind the point contact (neglected in the previous subsection), which we detect by a measurement of the thermovoltage across a second point contact situated in that region.

To increase the sensitivity of our experiment, we have used a low-frequency alternating current to heat the electron gas in the channel, and a lock-in detector tuned to the second harmonic to measure the root-mean-square amplitude of the thermovoltage $V_1 - V_4$. The voltages on the gates defining the second QPC were adjusted so that its conductance was $G = 1.5(2e^2/h)$. Finally, we applied a very weak magnetic field (15 mT) to avoid detection of hot electrons on ballistic trajectories from the first to the second point contact.

Figure 4*b*) shows a plot of the measured thermovoltage as a function of the voltage on the gates defining the point contact in the channel boundary, for a channel current of 0.6 μA (r.m.s. value). A sequence of plateaux is clearly visible, which line up with the quantized conductance plateaux of the point contact. Since the measured thermovoltage is directly proportional to δT, which in turn is proportional to the heat flow Q through the point contact, this result is a demonstration of the expected quantum plateaux in the thermal conductance $\kappa \equiv -Q/\Delta T$. We have verified that the second-harmonic thermovoltage signal at fixed gate voltages is proportional to I^2, as expected. Let us now see whether the magnitude of the effect can be accounted for as well.

To estimate the temperature increase $\delta T (\ll \Delta T)$ we write the heat balance for a region of area A

$$\kappa \Delta T = c_v A \delta T / \tau_\varepsilon \,. \tag{22}$$

We assume that the effective area A equals the square of the energy relaxation length $(D\tau_\varepsilon)^{1/2} \sim 10$ μm, so that τ_ε drops out of eq. (22). On inserting the (approximate) Wiedemann-Franz relation $\kappa \approx L_0 TG$, with $G = N(2e^2/h)$, and using the expression for the heat capacity per unit area given in the previous subsection (with $n_s = E_F m/\pi\hbar^2$), we find

$$\frac{\delta T}{\Delta T} \approx N \frac{\hbar}{mD} \,. \tag{23}$$

In the experiment $D = 1.4$ m^2/s, so that at the $N = 1$ plateau in the conductance we have $\delta T/\Delta T \approx 1.2 \cdot 10^{-3}$. The experimental curve in fig. 4*b*) was obtained at a current density in the main channel of $I/W_{ch} = 1.2$ A/m, close to that used in the thermopower experiment shown in fig. 3*b*). The analysis of the latter data indicated that $\Delta T \approx 2$ K at this current density. Consequently, $\delta T \approx 2$ mK. The point contact used as a thermometer (adjusted to $G = 1.5(2e^2/h)$) has $S \approx$ $\approx -40\,\mu$V/K (see subsect. 2·3), so that we finally obtain $V_1 - V_2 \approx -0.10\,\mu$V. The measured value is larger (cf. the first plateau in fig. 4*b*)), but not by more than 50%. All approximations considered, this is quite satisfactory.

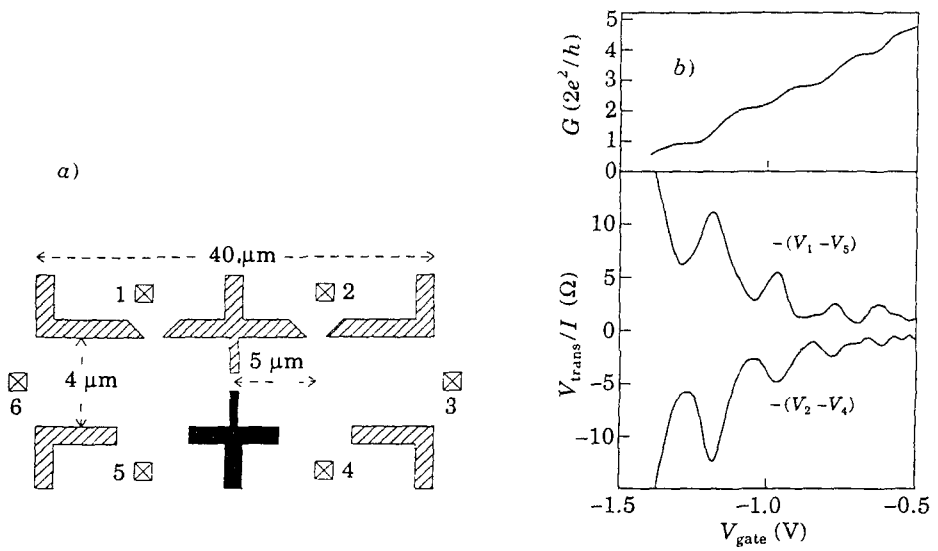

Fig. 5. – *a*) Layout of the device used to demonstrate quantum oscillations in the Peltier coefficient of a QPC. Positive current flows from Ohmic contact 6 to 3. The main channel is 4 μm wide, and the distance between the pairs of point contacts in its boundaries is 10 μm. *b*) Measured conductance and thermovoltages $-(V_1 - V_5)$ and $-(V_2 - V_4)$ divided by the current I as a function of the voltage on the (black) gate defining the point contact in the channel. The lattice temperature is 1.6 K and the current is about 0.1 μA near $G = 2e^2/h$. Gates defining point contacts 1 and 2 were adjusted so that their conductance was $G = 1.5\,(2e^2/h)$.

3·3. *Peltier effect.* – In this subsection we present results of an experiment designed to observe the quantum oscillations in the Peltier coefficient Π of a QPC. The geometry of the experiment is shown schematically in fig. 5*a*). A main channel, defined by split gates, is separated in two parts by a barrier containing a point contact. A positive current I passed from Ohmic contact 6, through this point contact, to Ohmic contact 3 is accompanied by a negative Peltier heat flow $Q = \Pi I$. The result is a temperature rise δT in the left-hand part of the channel, and a temperature drop δT in the right-hand part. These temperature changes of the electron gas can be detected by measuring the thermovoltages across additional point contacts in the channel boundaries—at least in principle.

A complication is that the changes in temperature δT come on top of an overall increase in temperature from the power dissipation I^2/G at the QPC in the channel. The dissipated power is not equally distributed among the 2DEG regions on either side, and it is precisely this imbalance which corresponds to the Peltier heat flow ΠI. We wish to detect only the temperature changes $\pm\,\delta T$ associated with the Peltier heat flow. This is accomplished by using an alternating current and a lock-in detector tuned to the fundamental frequency to measure

the components linear in I of the thermovoltages $V_1 - V_5$ and $V_2 - V_4$. (Note that the power dissipation produces a signal on the lock-in at twice the a.c. frequency.) The output voltage of the lock-in detector is divided by the current, to obtain a signal linearly proportional to the Peltier coefficient Π of the point contact in the channel. This signal, measured as a function of the voltage on (one of) the gates defining that point contact, should exhibit quantum oscillations, related to those seen in the thermopower S by the Onsager relation (2).

In order to adjust the central point contact without also affecting the QPC which measures the thermovoltage, we only vary the lower part of the central gate (the black gate in fig. 5*a*)). For the same reason, the device is designed such that the lithographic width (2 μm) of the split gates on the lower side of the channel is much larger than that on the top side of the channel (0.2 μm) (which define the thermometer point contacts). As a result, the thermopower of the contacts on the lower side of the channel is very small, so that a change in their width has a negligible effect on the transverse voltages $V_1 - V_5$ and $V_2 - V_4$. Results obtained at $I \sim 0.2$ μA and $T = 1.6$ K are plotted in fig. 5*b*), together with a trace of conductance *vs.* gate voltage for the point contact in the channel.

Oscillations in the thermovoltage (normalized by the current I) are clearly visible for both $-(V_1 - V_5)/I$ and $-(V_2 - V_4)/I$. The signals are of opposite sign, which proves that heating occurs in the left-hand part, and cooling in the right-hand part of the channel (for the current direction used). The oscillations have an amplitude up to ≈ 10 V/A and maxima aligned with the steps between conductance plateaux. The signals are linear in I and remain so for currents larger by at least one order of magnitude. Additional experiments at low magnetic fields have demonstrated that the signals are not sensitive to electrons travelling ballistically between the central and the thermometer point contacts. All this is consistent with the interpretation of the results in fig. 5*b*) as quantum oscillations in the Peltier coefficient Π.

Again, it is important to corroborate our interpretation by an estimate of the magnitude of the effect. To estimate the temperature rise (in the left-hand part of the channel) and decrease (in the right-hand part) of magnitude δT, we use again the heat balance equation. We find

$$\delta T \approx \frac{\Pi I}{c_v} \frac{\tau_\varepsilon}{A} . \tag{24}$$

To evaluate this expression, we use the Onsager relation $\Pi = ST$ (for $T = 1.65$ K), the theoretical value $S \approx -40$ μV/K (for $G = 1.5(2e^2/h)$) and the value $\tau_\varepsilon \sim 10^{-10}$ s deduced from the thermopower experiments described above. Since the length of the channel W_{ch} in the present sample (20 μm on either side of the central point contact) is larger than the energy relaxation length $(D\tau_\varepsilon)^2$ (in contrast with the situation in the sample used to measure the thermal

conductance), we estimate the area A as the product of these quantities, $A = (D\tau_\varepsilon)^{1/2} W_{ch} \sim 50\ \mu m^2$. Thus we find that $\partial T/I \approx 10^5$ K/A. The resulting thermovoltage across one of the thermometer point contacts (adjusted to $G = 1.5\,(2e^2/h)$ as well), normalized by I, would then be about 4 V/A, in reasonable agreement with the experimentally observed amplitude of ~ 10 V/A.

4. – Conclusions.

In conclusion, we have reviewed the theory of the thermal and thermo-electric effects in a quantum point contact [6-8] and our experiments on the quantum oscillations in the thermopower [10]. Data have been presented that show the quantum steps in the thermal conductance and the quantum oscillations in the Peltier coefficient. Our experiments exploit quantum point contacts as miniature thermometers. The results for the thermal and thermo-electric transport coefficients presented here compare reasonably well with the theoretical estimates based on a simple heat balance argument. A full account of our experiments on thermal conductance and Peltier effect is published elsewhere [15].

* * *

We acknowledge valuable contributions of M. J. P. BRUGMANS, R. EPPENGA, TH. GRAVIER and M. A. A. MABESOONE at various stages of this work, and thank H. BUYK and C. E. TIMMERING for their technical assistance. The support of M. F. H. SCHUURMANS is gratefully acknowledged. This research was partly funded under the ESPRIT basic research action project 3133.

APPENDIX

In this appendix we outline the derivation of the expressions (7)-(9) for the transport coefficients, for the two-terminal geometry shown in fig. 6. (More general multi-terminal derivations are given in ref. [6] and [7].) Figure 6 repre-

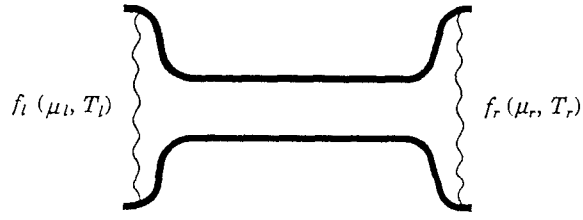

Fig. 6. – Illustration of thermo-electric transport through an ideal electron waveguide connected adiabatically to two reservoirs l and r, having electrochemical potentials μ_l and μ_r, temperatures T_l and T_r, and Fermi distributions f_l and f_r.

sents an ideal electron waveguide, connected adiabatically to two reservoirs l and r, which have electrochemical potentials μ_l and μ_r and temperatures T_l and T_r, respectively. The reservoirs are in thermal equilibrium, and are described by Fermi functions f_l and f_r (eq. (10)). The transmission probability at energy E through the waveguide (summed over the 1D subbands) is given by the function $t(E)$ (which increases stepwise with energy E). As a result of the cancellation of group velocity and density of states for a 1D subband [3], the current through the electron waveguide is

$$I = -\frac{2e}{h}\int_0^\infty \mathrm{d}E\,(f_l - f_r)\,t(E)\,. \tag{A.1}$$

The heat current Q is given by a similar expression as I, but with an additional factor $E - E_F$ in the integrand:

$$Q = \frac{2}{h}\int_0^\infty \mathrm{d}E\,(f_l - f_r)\,t(E)(E - E_F)\,. \tag{A.2}$$

To obtain the transport coefficients in linear response, we expand f_l and f_r to first order in $\Delta\mu = \mu_r - \mu_l$ and $\Delta T = T_r - T_l$, to obtain

$$f_l - f_r \approx \frac{\partial f}{\partial E}\left(\Delta\mu + \frac{E - E_F}{T}\,\Delta T\right). \tag{A.3}$$

Substitution of eq. (A.3) in eqs. (A.1) and (A.2), and a comparison with the definitions in eq. (1), yields eqs. (7)-(9), for the transport coefficients.

REFERENCES

[1] B. J. VAN WEES, H. VAN HOUTEN, C. W. J. BEENAKKER, J. G. WILLIAMSON, L. P. KOUWENHOVEN, D. VAN DER MAREL and C. T. FOXON: *Phys. Rev. Lett.*, **60**, 848 (1988).

[2] D. A. WHARAM, T. J. THORNTON, R. NEWBURY, M. PEPPER, H. AHMED, J. E. F. FROST, D. G. HASKO, D. C. PEACOCK, D. A. RITCHIE and G. A. C. JONES: *J. Phys. C*, **21**, L209 (1988).

[3] A comprehensive review of quantum transport in semiconductor nanostructures is C. W. J. BEENAKKER and H. VAN HOUTEN: *Solid State Phys.*, **44**, 1 (1991).

[4] R. LANDAUER: *IBM J. Res. Dev.*, **1**, 223 (1957).

[5] M. BÜTTIKER: *Phys. Rev. Lett.*, **57**, 1761 (1986).

[6] U. SIVAN and Y. IMRY: *Phys. Rev. B*, **33**, 551 (1986).

[7] P. N. BUTCHER: *J. Phys. Condensed Matter*, **2**, 4869 (1990).

[8] P. STREDA: *J. Phys. Condensed Matter*, **1**, 1025 (1989).

[9] Current heating has also been used in a study of fluctuations in the thermopower in the phase-coherent diffusive transport regime by B. L. GALLAGHER, T. GALLOWAY, P. BETON, J. P. OXLEY, S. P. BEAUMONT, S. THOMS and C. D. W. WILKINSON (*Phys. Rev. Lett.*, **64**, 2058 (1990)).

[10] L. W. MOLENKAMP, H. VAN HOUTEN, C. W. J. BEENAKKER, R. EPPENGA and C. T. FOXON: *Phys Rev. Lett.*, 65, 1052 (1990).
[11] L. W. MOLENKAMP, H. VAN HOUTEN, C. W. J. BEENAKKER, R. EPPENGA and C. T. FOXON: in *Condensed Systems of Low Dimensionality, NATO ASI Series B* 253, edited by J. BEEBY (Plenum, New York, N.Y., 1991), p. 335.
[12] H. VAN HOUTEN, L. W. MOLENKAMP, C. W. J. BEENAKKER and C. T. FOXON: in *Proceedings of the 7th International Conference on Hot Carriers in Semiconductors, Semicond. Science Technol.*, 7, B215 (1992).
[13] S. R. DE GROOT and P. MAZUR: *Non-Equilibrium Thermodynamics* (Dover, New York, N.Y., 1984).
[14] J. J. HARRIS, J. A. PALS and R. WOLTJER: *Rep Prog. Phys*, 52, 1217 (1989).
[15] L. W. MOLENKAMP, TH. GRAVIER, H. VAN HOUTEN, M. A. A. MABESOONE, O. J. A. BUIJK and C. T. FOXON: *Phys. Rev. Lett.*, 68, 3765 (1992).